Axial Behavior of Carbon Nanofiber Enhanced UHPC Rectangular Columns

Milana Cimesa – PhD Candidate, University of Nevada, Reno, Civil and Environmental Engineering, Reno, NV, USA, Email: mcimesa@nevada.unr.edu

Mohamed A. Moustafa, Ph.D., P.E. (corresponding author) – Associate Professor, University of Nevada, Reno, Civil and Environmental Engineering, Reno, NV, Email: mmoustafa@unr.edu

Abstract

Advanced materials, such as UHPC, are among the emerging technologies that can revolutionize our future structures with significantly improved strength and durability for a much longer service life compared to conventional concrete. Behind the excellent performance of UHPC stands its dense packing theory which excludes the usage of coarse aggregates and incorporates steel fibers in order to bridge the microcracks and provide high post-cracking strength and ductility. Emerging UHPC mixtures may also contain carbon nanofibers (CNFs) that further enhance the nanostructure of UHPC and its cracking behavior. Most traditional and CNF-enhanced UHPC applications are still bridge field joints and other small-scale applications. Exploring the behavior and the design of robust UHPC mixtures with CNFs when used in full structural components will provide the understanding and the tools to expand the use of UHPC in large structural applications or full systems. Due to the lack of a comprehensive database on full-scale UHPC columns, especially CNF-enhanced UHPC columns, this research study provides a first look at the transverse reinforcement detailing effects on the structural behavior and deformation capacity of four full-scale UHPC rectangular columns tested at the 4000-kip machine at UC Berkeley under axial loading. The paper discussion is concerned mainly with presenting and interpreting the axial behavior of the CNF-enhanced UHPC columns, but with particular focus on effect of ACI- and non-ACI compliant transverse reinforcement detailing in rectangular columns.

Keywords: carbon nanofibers, steel fibers, confinement, axial behavior, full-scale testing, precast columns, transverse reinforcement details

Introduction

Even though ultra-high performance concrete (UHPC) has the features of a mortar, it is widely known and excepted as concrete. Behind the excellent performance of this type of concrete stands its dense packing which excludes the usage of coarse aggregates and incorporates steel fibers in order to bridge the microcracks and provide high post-cracking tensile strength with the increase of ductility, avoiding the brittleness of the concrete (Abokifa and Moustafa 2022). Compressive strength of UHPC can be four to six times higher, while tensile strength is approximately two times higher when compared to normal strength concrete (NSC) (Graybeal 2014). Although all these features are promising to be used in diverse applications, this type of concrete is mainly used in bridge construction, mostly as small structural elements such as field joints, deck panels, and girders, due to its high cost, lack of comprehensive knowledge on the process of the mixing and absence of design guidance applicable for this type of material (Graybeal 2014).

Due to the superior properties and performance of UHPC, many research studies are investigating the behavior of this type of concrete for various applications as well as exploring

new technologies in UHPC. For example, a recent study by the authors (Cimesa and Moustafa 2022) aimed at investigating the behavior of carbon nanofiber (CNF)-enhanced UHPC cylinders under compressive loading. More than 230 unconfined and confined 3 × 6 in (75 × 150 mm) cylinders were tested. The variables in that experimental campaign included transverse reinforcement ratios (0, 2, and 4 %) and steel fiber ratios (0-4 %) at a constant CNF ratio throughout the batches (0.5% by volume). The study provided full characterization of CNF-enhanced UHPC compressive stress-strain relationship and modulus of elasticity at different ages. Furthermore, the study showed that CNF can further enhance the post-peak ductile behavior in cylinders properly confined by transverse reinforcement and steel fibers. Cimesa and Moustafa (2022) also found that current analytical models, based on Naeimi and Moustafa (2021) for conventional UHPC, do not precisely predict the behavior of this novel type of UHPC.

Although there are several research studies on UHPC columns (e.g. Aboukifa and Moustafa 2021; 2022), there is still a need for more experimental data to explore emerging UHPC types and develop proper design guidelines for larger structural applications. There is insufficient knowledge, for instance, to quantify CNFs or steel fibers effects on confinement and how it relates to optimum amount of transverse reinforcement for full structural UHPC columns. Therefore, this research study aims to provide exclusive experimental data for CNF-enhanced UHPC and further understand the behavior of full-scale UHPC columns under compressive loading. In order to fill some of the knowledge gaps identified above, four 9-ft (2.74 m) tall columns were tested under concentric axial compressive loading. The main objectives of this study are to (1) capture the mechanical properties of four CNF-enhanced UHPC rectangular columns with respect to varying reinforcement detailing, (2) investigate the columns' axial stiffness, and (3) assess proper capacity estimation factors for both non-ACI and ACI compliant UHPC columns.

Experimental Program

Four columns are presented in this research study, which were part of a larger experimental program and ACI-sponsored project that tested 13 UHPC columns. All 13 UHPC columns, with different UHPC mixtures, were constructed at the Earthquake Engineering Laboratory fabrication yard at the University of Nevada, Reno (UNR). After the construction and curing, all columns were transported and tested at UC Berkeley PEER Structural laboratory. In particular, the four columns whose behavior is analyzed in this study were constructed using CNF-enhanced UHPC.

2.1. Material Properties and the Construction of the Columns

All four columns were constructed from a commercial UHPC mixture containing CNFs made by ceEntek. The unique component of this type of UHPC is a thick black-colored paste containing dispersed carbon nanofibers mixed with admixtures. The features of the carbon nanofiber paste are shown in Figures 1a and 1b. According to the vendor's specifications, the CNFs volumetric ratio is 0.5% by volume, which was same for all mixing batches. In general, the CNFs fill the nanopores, preventing nano cracks from propagating into the micro-cracks (Cimesa and Moustafa 2022). Besides the CNF paste at 0.8 lb/ft^3 (132 kg/m^3), the main ingredients of the UHPC used in this study are: (1) preblended, prebagged dry mix ingredients (fine sand and pozzolanic material, and cement) at 143.6 lb/ft^3 (2300 kg/m^3); (2) water at 10.1 lb/ft^3 (161 kg/m^3); (3) calcium nitrate accelerator as 70% liquid at 1.4 lb/ft^3 (23 kg/m^3); and (4) steel fibers at 9.7 lb/ft^3 (156 kg/m^3). According to the vendor's datasheet, the diameter and length of the steel fibers are 0.008 and 0.5 in (0.2 and 12.7 mm), respectively, with a yielding stress of 400 ksi (2751 MPa).

The mixing of all mentioned ingredients lasted from 20 to 45 minutes. First, the dry mix was added slowly into an Imer Mortman 360 high-shear mixer. After one minute of mixing, the water previously mixed with the admixtures was added to the dry mix. When the right consistency was achieved, steel fibers were added and mixed with the rest of the ingredients for only one minute to avoid segregation of the steel fibers on the bottom of the mixer. When the mixing was done, the concrete was poured into the columns' formwork positioned horizontally, as shown in Figure 1c.

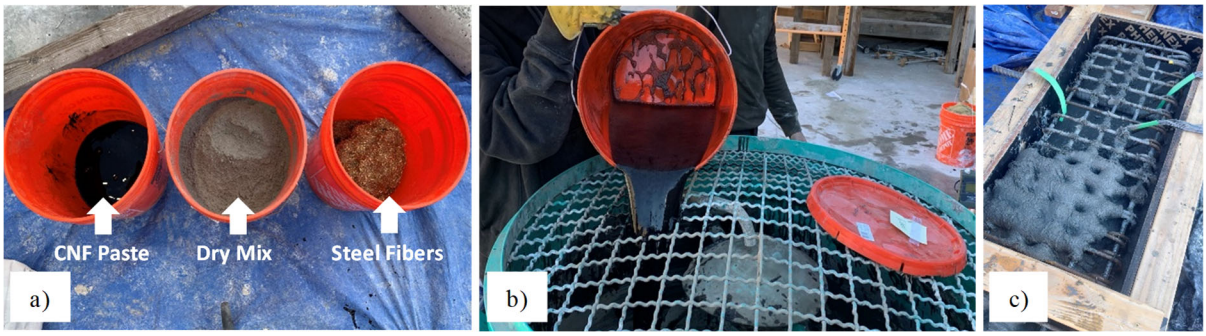

Figure 1. (a) CNF-enhanced UHPC ingredients, (b) adding CNF paste to mixture, and (c) casting of column

In order to try to prevent water evaporation/freezing after the casting day due to the temperature oscillations during the day and freezing temperatures over the night in Reno during winter time, all columns were covered by heat blankets for approximately two weeks. The heat blankets partially helped prolong the hydration and prevent the freezing of the water particles. It is worth mentioning that the rebar cages were instrumented with strain gages on selected longitudinal and transverse reinforcement bars to capture the compressive and tensile strain propagation on more than 20 locations throughout each column. Moreover, to capture the progression of the strength over time and on the test day, which is approximately a time period of seven months since the casting of concrete, at least six cylinders per column were poured and placed alongside to go through the same temperature cycles as the columns.

2.2. Test Matrix

The test matrix shown in Table 1 was designed to investigate the behavior of the UHPC columns under compressive loading in terms of axial strength, compressive strain, and stiffness while having different transverse reinforcement ratios (variation in spacing and detailing configuration). As mentioned earlier, the four columns used in this study were 9 ft (2.74 m) in height with rectangular cross-section dimensions 10 × 16 in (254 × 406 mm) and made out of CNF-enhanced UHPC. It is worth noting that all columns used in this study are categorized as non-slender columns according to the ACI 318-19 provision.

From Table 1, it is noted that transverse reinforcement configuration varied among the columns. Current ACI standards do not yet provide guidelines for UHPC design, and design codes meant for NSC are not necessarily appropriate for UHPC. For example, ACI 318-19 overestimates the axial load capacity of the columns (Cai et al. 2021). Also, for seismic columns, using the ACI 318-14 equations would require more than 10% of transverse reinforcement ratio for UHPC columns with high strength values, which is not feasible and confirm that such equations are not suitable for UHPC. In this research study, the test matrix considered in some cases ACI-compliant reinforcement detailing where no unsupported longitudinal rebar with lateral tie spacing exceeding 6 in (150 mm). Also, the longitudinal spacing of the transverse reinforcement compliant columns was limited to 2.5 in (63.5 mm) to avoid buckling between two hoops. Therefore, the test matrix included two properly (SP-2 and SP-4) and two non-properly (SP-1 and SP-3) confined columns.

Table 1 – Reinforcement configuration of four carbon nano-enhanced UHPC (SP stands for specimen)

Column ID	Longitudinal Reinforcement	Transverse Reinforcement
SP-1	12 # 4 (ø 13)	ø 10 (# 3) at 2.5 in (63.5 mm)
SP-2	12 # 4 (ø 13)	ø 10 (# 3) at 2.5 in (63.5 mm) w/ internal hoop & crosstie
SP-3	12 # 4 (ø 13)	ø 10 (# 3) at 5 in (127 mm)
SP-4	12 # 4 (ø 13)	ø 10 (# 3) at 2.5in (63.5 mm) w/ one crosstie

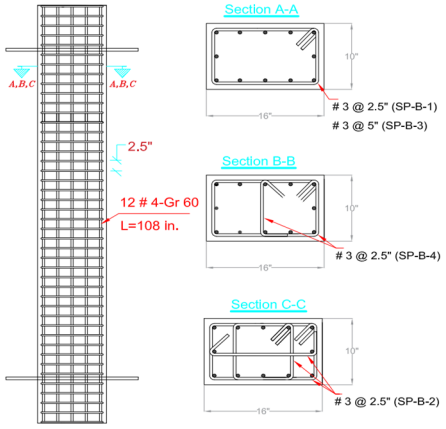

All columns were reinforced by A706 Grade 60 (420) longitudinal and transverse rebars. Dedicated tensile tests were performed on #3 and #4 (ø10 and ø16) rebar coupons to determine the actual tensile behavior but results are not shown here for brevity.

2.3. Construction Challenges

Some challenges occurred during the construction of some of the columns, which later showed some impact on tested structural behavior. Five batches were needed to construct each of the four columns. Due to the high dosage of the accelerator and the cold weather in Reno during construction, some specimens had almost four cold joints due to the quick setting time of the previously mixed and cast layer. Mixing each of the five batches lasted 20-30 minutes more than anticipated. The previous cast layer was already hardening when the fresh batch of concrete was poured, preventing proper intermixing between the layers. As a result of poor connections between the layers, delamination of four layers was observed later after the end of the testing as shown in Figure 2. Furthermore, due to the relatively lower flowability of UHPC with high accelerator dosage, minor honeycombing was observed in SP-1 and SP-2 after taking the formwork off (see Figure 2). Due to the high percentage of transverse reinforcement, and low flowability, a high percentage of the steel fibers could not pass through the dense reinforcement configuration. Consequently, the steel fibers could not be uniformly dispersed over the height of the column. According to Sbia et al. (2014), the relatively large spacing of the fibers lead to microcracks expansion, which was also observed in some columns as discussed later and shown in Figure 2.

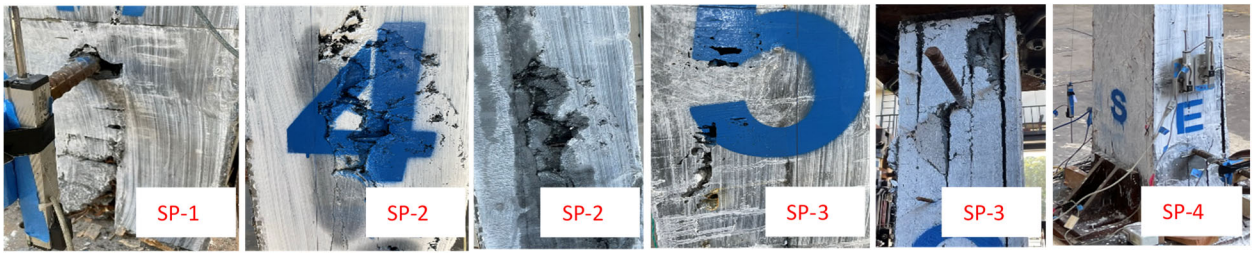

Figure 2. Honeycombs and delamination of all four columns

Furthermore, according to Du et al (2021) and Heshe and Nielsen (1992), the direction of the pouring UHPC may have a significant effect. As mentioned earlier, the columns tested in this study were horizontally placed to represent typical precast settings, and in turn, the pouring of concrete was perpendicular to the loading direction. Considering the steel fibers' orientation, the pouring direction should be parallel to the loading direction. In this study, however, steel fibers, due to the

pouring, were mostly orthogonal to the loading direction, which may lower the bridging effect at the time of the crack openings. The orientation of steel fibers may not distress other columns significantly. Thus, in the specimens that already experienced some construction challenges, the obtained steel fiber orientation added additional adverse effects on the overall behavior.

3. Test Results and Discussion

3.1. Summary of Results

Table 2 provides an overall summary of maximum axial load capacity, strain at peak force, and estimated stiffness for all 4 columns. It is noted that per the proper reinforced detailing explained earlier, SP-1 and SP-3 had less transverse reinforcement, while SP-2 had more when assessed against ACI detailing requirements. Only SP-4 followed the proper reinforcement detailing requirements. SP-1 had a 2.5 in (63.5 mm) spacing without any additional hoops or ties. SP-3 had the same transverse rebar configuration as SP-1 but with 6 in (152 mm) longitudinal hoop spacing. The heavily reinforced column, SP-2, had rectangular hoops and crossties tying the middle bars on the opposite sides of the shorter dimension using 2.5 in (63.5 mm) spacing, as shown earlier on the elevation view in Table 1. Similarly, the transverse reinforcement configuration of SP-4 had crosstie on the longitudinal rebar due to more than 6 in (152 mm) space between the corner and middle bars (ACI 318 requirement).

Table 2 – Summary of key test results of all four CNF-enhanced UHPC columns

Column ID	Cross-section Area in^2 (cm^2)	Max. Axial Force kips (kN)	Strain at Peak	Stiffness kip/in (kN/mm)
SP-1	170.6 (1,101.0)	1,796 (7,990)	0.002579	11,832 (2,072)
SP-2	163.3 (1,053.8)	2,503 (11,134)	0.002857	12,487 (2,187)
SP-3	168.7 (1,088.2)	2,186 (9,723)	0.002507	11,842 (2,074)
SP-4	167.9 (1,083.2)	2,770 (12,320)	0.002894	12,844 (2,249)

3.2. Damage Progression

Specimens' modes of failure are presented above in Figure 2 and discussed first in the context of some of the construction challenges. For testing, all specimens were subjected to the axial concentric loading up to the complete loss of the columns' axial capacity. During the loading process, it was observed that columns had some minor crushing of concrete at the top and the bottom. These crashing signs were due to imperfections during the construction (various lengths of the longitudinal rebars). These imperfections led to minor eccentricity effects.

The first major damage was the spalling of the cover concrete, visually noticeable by the vertical splitting of the concrete and the reduction in load resistance. Due to the higher compressive force, only in SP-1, one of the transverse bars subjected to the high tensile strain was getting gradually more soft and incapable of providing confining stress to the core concrete. At the end of the testing, transverse reinforcement was fractured under the high tensile stresses at the failure load due to the crack openings and the local buckling effect of the longitudinal rebar.

The honeycomb observed in SP-1 and SP-2 reduced the cross-section in some of the columns' areas. These reduced sections and holes led to some local stress concentration leading these two specimens to premature failures. Also, as shown in Figure 2, SP-3 and SP-4 had delamination issues. The improper connection between all five layers was the main damage pattern in both specimens. Even though the delamination affected the failure modes, both columns achieved high axial capacity compared to the rest of the specimens.

3.3. Force versus Deformation and Strain Relationships

Figure 3 provides the force-deformation relationship as captured for each column using three different measurements using string pots (SP) between base and loading head as well as LVDTs between installed big rods (BR) and small instrumentation rods (SR). The average curves from all measurements are shown as well. According to the force versus deformation relationships shown in Figure 3, the stiffnesses of all four columns was almost similar. Analyzing the failure mode and the results gathered through the strain gages for specimen SP-1, it can be observed that only one longitudinal bar yielded while the rest did not. This may be due to the eccentricity that led to the failure of one of the transverse reinforcements causing the local buckling effect and loss of capacity. However, the columns' deformation kept increasing under the constant load. This may be due to the resistance provided by the other longitudinal rebars.

Figure 4 compares the average obtained axial strain for all columns. As shown in Figure 4, SP-1 had the highest axial strain capacity with the lowest failure load. Due to the better flowability and fewer observed honeycombs on the surface, SP-3 and SP-4 performed well in terms of the achieved failure load. Also, SP-2 exhibited high axial strain capacity, which was expected due to over-confinement. It is noted again that the lower compressive stress capacity of SP-2 may be due to the steel fibers uneven dispersion over the height, low flowability, and honeycombing.

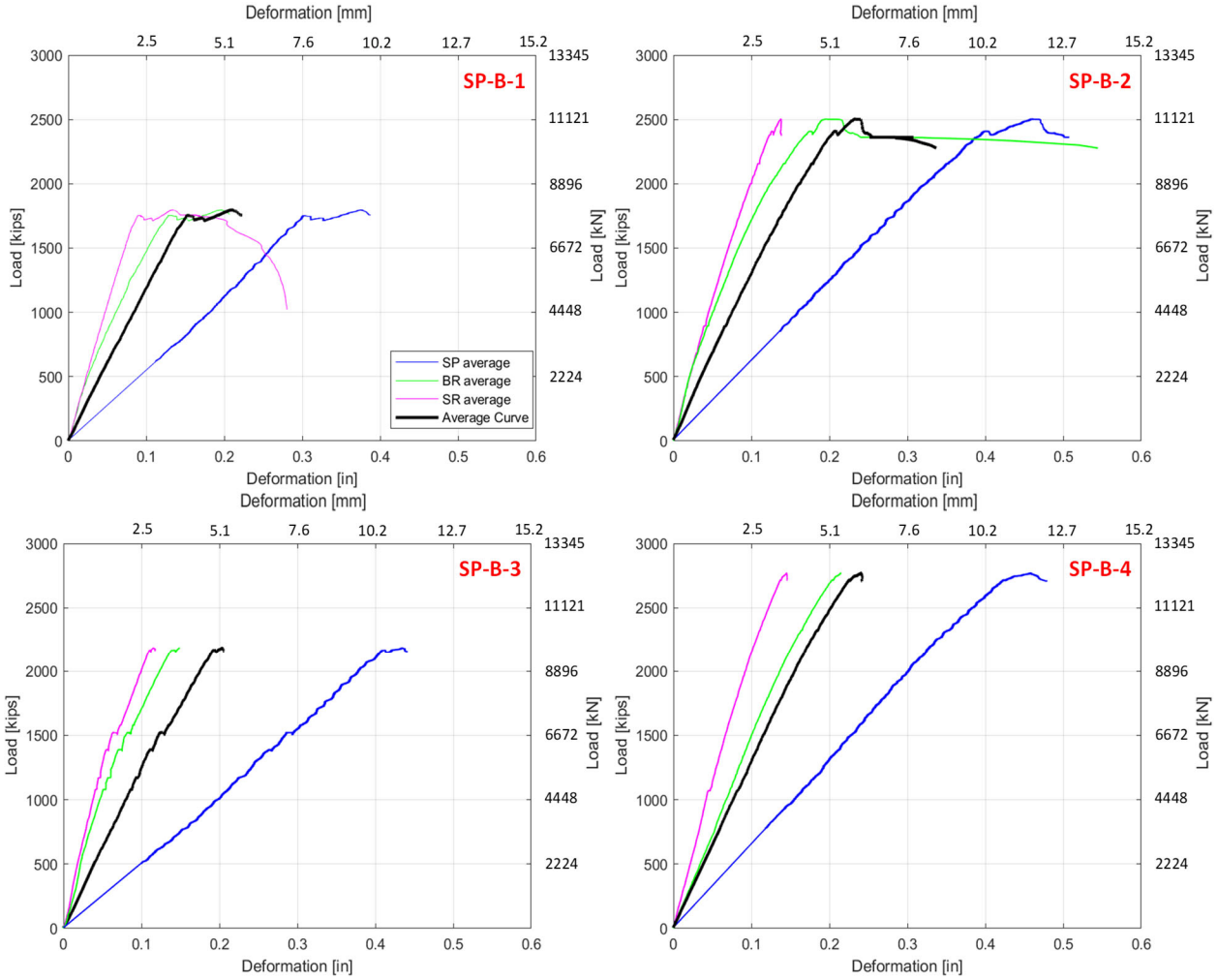

Figure 3. Axial force versus deformation relationships for all columns using different measurements

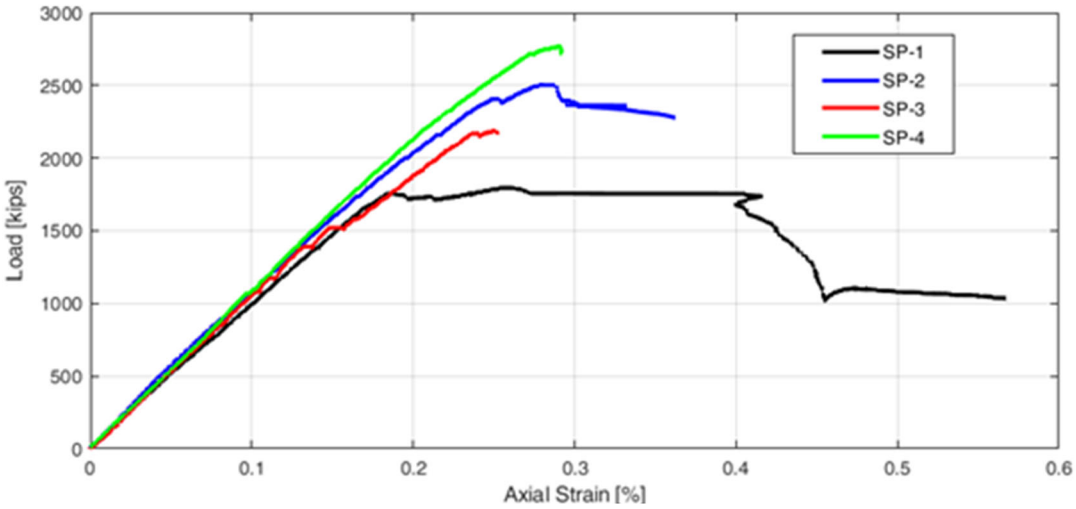

Figure 4. Average curves of axial force versus axial strain for all four CNF-enhanced UHPC columns

4. Axial Load Capacity Reduction Factor

A strength reduction factor, labeled as α, is used in Equation (1) for axial strength with no eccentricity, when multiplied by the strength of the companion cylinder, presents the actual compressive strength of the structural element and accounts for the uncertainties due to the difference in the size, shape, casting of the specimens, etc. Besides strength reduction, Equation (I) incorporates values for f_c' - cylinders' modulus of elasticity, A_g - gross cross-section area of the column, A_s - the area of the longitudinal reinforcement, and f_s - yielding stress of the steel. According to ACI318-19, for NSC the reduction factor should be 0.85. On the other hand, according to [9], the proposed value of this factor is 0.75. As noted before, most of the columns in this research study had some level of eccentricity. According to ACI 318-19, the nominal strength capacity should be reduced by a 0.8 factor when considering accidental eccentricity. Therefore, the reduction factors of 0.85 and 0.75 proposed by ACI and Aboukifa and Moustafa (2022) would overestimate the axial strength of the columns with recorded eccentricity. In this research study, according to Table 3, the nominal capacity of properly confined columns is approximately 0.60, which is a justified value when the accidental eccentricity factor is added to the 0.75 factor found by Aboukifa and Moustafa (2022) specifically for the UHPC columns. Furthermore, for the non-properly reinforced columns (SP-1 and SP-3), the reduction factor is calculated to be 0.46, as presented in Table 3.

$$P_o = \alpha f_c'\left(A_g - A_s\right) + A_s f_s \tag{1}$$

Table 3 – The maximum strength of the cylinders, strain at peak, rebar strength at the yielding, maximum applied force to the columns, and reduction factor for properly and non-properly confined columns

Column ID		f_c' (ksi)	ε	f_s (ksi)	P_{max} (kips)	α
Properly Confined	**SP-2**	24.23	0.0022	62.93	2503.13	0.60
	SP-4	26.11	0.0022	64.87	2769.57	0.60
					average	0.60
Non-properly Confined	**SP-1**	23.71	0.0014	40.81	1796.26	0.43
	SP-3	24.51	0.0019	53.82	2185.75	0.50
					average	0.46

f_c': cylinders strength, ε: strain at peak, f_s : yielding stress of steel, P_{max}: maximum applied force

5. Conclusions

In this study, four full-scale CNF-enhanced UHPC columns were tested under pure axial load. The overall goal of this paper was to analyze the behavior in terms of force versus axial deformation and force versus axial strain of the 9-ft tall columns with respect to varied transverse reinforcement. Few concluding remarks can be drawn from this work as follows:

- Due to the relatively high percentage of accelerator used for mixing, lower flowability and faster hardening was observed leading to some construction challenges.
- The orientation of steel fibers may not distress columns significantly, but in the specimens that were already exposed to some construction challenges, the "not-so-ideal" steel fiber orientation may add additional adverse effects on the overall mechanical behavior of those specimens.
- The strength reduction factor for the properly confined columns is proposed to 0.60, while non-properly confined columns can use a lower reduction factor of 0.46 for capacity estimation, noting that both factors directly account for the 0.8 reduction for accidental eccentricity.

References

- Abokifa, M., M.A. Moustafa, (2021). "Mechanical Characterization and Material Variability Effects of Emerging Non-Proprietary UHPC Mixes for Accelerated Bridge Construction Field Joints", Construction and Building Materials, 308, 125064
- Aboukifa, Mahmoud, and Mohamed A. Moustafa. "Reinforcement detailing effects on axial behavior of full-scale UHPC columns." Journal of Building Engineering 49 (2022): 104064.
- Aboukifa, M., M.A. Moustafa, (2021). "Experimental Seismic Behavior of Ultra-High Performance Concrete Columns with High Strength Steel Reinforcement", Engineering Structures, 232, 111885
- Cai, Heng, et al. "Seismic performance of rectangular ultra-high performance concrete filled steel tube (UHPCFST) columns." Composite Structures 259 (2021): 113242.
- Cimesa, M., and M.A. Moustafa. "Experimental characterization and analytical assessment of compressive behavior of carbon nanofibers enhanced UHPC." Case Studies in Construction Materials, 17 (2022): e01487.
- Du, Jiang, et al. (2021) "New development of ultra-high-performance concrete (UHPC)." Composites Part B: Engineering, 224 (2021): 109220.
- Graybeal, Ben. Design and construction of field-cast UHPC connections. No. FHWA-HRT-14-084; HRDI-40/10-14 (750) E. United States. Federal Highway Administration, 2014.
- Heshe, Gert, Nielsen CV, (1992). "Behavior in compression, triaxial stress state and short columns." Report EU264-Compressit Aalborg Portland, Aalborg,51p.
- Naeimi, N., M.A. Moustafa, (2021). "Analytical Stress-Strain Model for Steel-Spiral Confined UHPC", Composites Part C: Open Access, 5, 100130
- Sbia, Libya Ahmed, et al. "Enhancement of Ultrahigh Performance Concrete Material Properties with Carbon Nanofiber." Advances in civil engineering (2014).
- Yoo, Doo-Yeol, Taekgeun Oh, and Nemkumar Banthia. "Nanomaterials in ultra-high-performance concrete (UHPC)–A review." Cement and Concrete Composites (2022): 104730.